JOURNAL OF MATERIALS SCIENCE 17 (1982) 3057–3065

X-ray powder diffraction evidence for the incorporation of W and Mo into $M_{23}C_6$ extracted from high-temperature alloys

F. J. FRANCK, P. TAMBUYSER, I. ZUBANI
Commission of the European Communities, Joint Research Centre, Petten Establishment, Postbus 2, 1755 ZG Petten, The Netherlands

X-ray powder diffraction patterns of $M_{23}C_6$ where M=(Cr, Mo) and M=(Cr, W) have been recorded accurately using a focusing Guinier camera and a diffractometer. The improved resolution of the modern focusing diffraction equipment made it possible to detect new features in the powder diffraction patterns, showing that $M_{23}C_6$ carbides extracted from W- and Mo-containing alloys differ from pure $Cr_{23}C_6$ and $(Cr, Fe)_{23}C_6$ met in more conventional stainless steels. The distinctions concern the lattice parameters, as well as the intensities of specific diffraction maxima. These differences can be explained in terms of the theoretical considerations of Goldschmidt who predicted that W and Mo, when incorporated in $Cr_{23}C_6$, will preferentially occupy specific positions in the unit cell. Diffraction intensity calculations indeed confirm that the introduction of W and Mo atoms on these particular positions will modify the diffracted intensities in the same way as was observed experimentally.

1. Introduction

X-ray powder diffraction measurements on precipitates extracted from chromium-containing superalloys and austenitic stainless steels frequently reveal the presence of $M_{23}C_6$ type carbides. M usually stands for Cr and Fe, but it is known that these carbides may also contain larger atoms such as W or Mo [1]. This will actually be the case when small amounts of these solution-hardening elements are added to an alloy in order to improve its strength [2, 3].

The crystal structure of $M_{23}C_6$ is known in detail and a crystallographic study led Goldschmidt [4] to predict that Fe, W or Mo, when incorporated into $M_{23}C_6$, will preferentially occupy specific positions in the unit cell. The literature, however, does not mention the possible influence the heavy atoms can have on the X-ray powder diffraction pattern and no detailed descriptions of diffractographs of W or Mo containing $M_{23}C_6$ were found.

The present paper, therefore, reports on X-ray powder diffraction pattern calculations showing that the introduction of W and Mo on particular positions in the unit cell of $M_{23}C_6$ will measurably affect the intensities, but that Fe has hardly any influence on the intensity pattern. Experimental X-ray powder diffraction patterns of $Cr_{23}C_6$, $(Cr, Fe)_{23}C_6$, $(Cr, W)_{23}C_6$ and $(Cr, Mo)_{23}C_6$ will be seen to confirm these results.

2. The crystallography of $M_{23}C_6$

The crystal structure of $Cr_{23}C_6$ (Fig. 1) has been determined by Westgren [1] in 1933. The unit cell of the carbide can be subdivided into eight cubic octants, the corners of which are alternately surrounded by metal atoms in a cubo-octahedral (Fig. 1b) and in a simple cubic configuration (Fig. 1c). Following Wyckoff's notation the positions of the atoms that build the cubo-octahedra and the cubes are called h-positions and f-positions, respectively. Additional metal atoms occupy the centre of each cubo-octahedra (a-positions) (Fig. 1e) and the more spacious centre of each octant (c-positions) (Fig. 1f). The carbon atoms are located on e-positions (Fig. 1d).

0022–2461/82/103057–09$03.58/0

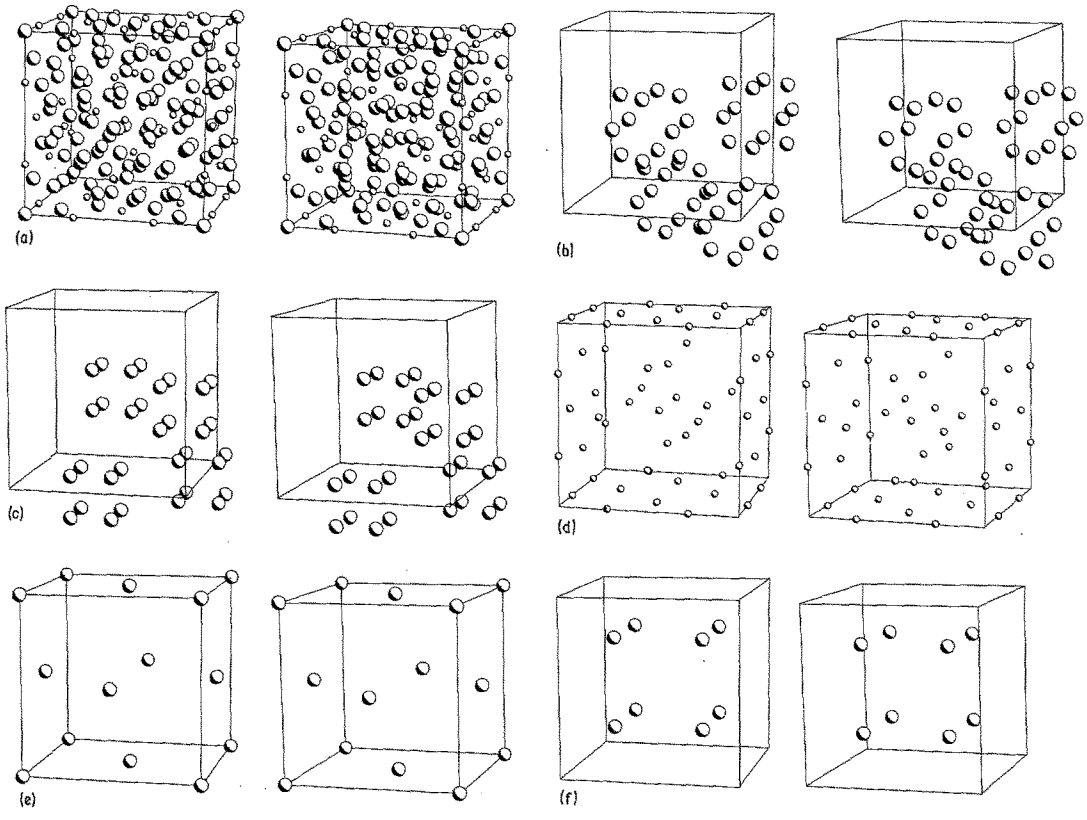

Figure 1 Stereographic representation of the crystal structure of $M_{23}C_6$. (a) The complete cell. (b) Cr-atoms on h-positions forming cubo-octahedra. (c) Cr-atoms on f-positions forming simple cubes. (d) Cr-atoms on e-positions. (e) Cr-atoms on a-positions at the centres of the cubo-octahedra. (f) Cr-atoms on c-positions.

To each of these positions corresponds a specific co-ordination of neighbour atoms. As far as the metal atoms are concerned, Westgren [1] pointed out that the c-positions are the most spacious and that the f-positions are the most restricted.

Combining this knowledge with experimental evidence and with the fact that Fe atoms have a smaller atomic radius than Cr, (Table I), Goldschmidt [4] concluded that starting from pure $Cr_{23}C_6$, iron can replace chromium quite extensively in such a way that the Fe-atoms will preferentially occupy the cubic f-positions. Up to about 30 at.% Cr can thus be substituted by Fe when all the available space is occupied. Upon excess substitution of Cr by Fe, the octant centres (c) would become too spacious to continue taking chromium only and a larger atom W or Mo is required to fill them, in order to enable the carbide to dissolve more Fe. Concerning the X-ray powder diffraction of $Cr_{23}C_6$, most of the literature data [5–8] have been collected in the Powder Diffraction File (PDF) of the JCPDS – International Centre for Diffraction Data [9]. It is noticed that these data primarily refer to pure $Cr_{23}C_6$. The values for the intensities on the relevant PDF cards have been obtained as visual estimates from photographic recordings. A common feature of the different patterns is the absence of {111}, {200}, {220}, {444}, {642} and {842} reflections. Specific data on W and Mo containing $M_{23}C_6$ are scarce and no detailed descriptions of corresponding patterns were found. Neither does the literature give any indication that a particular difference with respect to $Cr_{23}C_6$ might exist.

TABLE I Atomic number, weight and radius (nm) of elements encountered in $M_{23}C_6$ [18]

	Cr	Fe	Mo	W
Atomic number	24	26	42	74
Atomic weight	52.0	55.8	95.9	183.9
Atom radius	0.128	0.127	0.140	0.141

3. Experimental details

3.1. Intensity calculations

Computed X-ray powder diffraction patterns

were obtained with an unpublished computer program called CRYDIF. This program was written in Fortran IV for a PDP 11 under RSX-11M. It can be used to calculate interplanar spacings, structure factors and diffracted intensities for purposes of X-ray and electron diffraction. Basically the program requires the input of the type of radiation, the crystal system, the lattice parameters and individual Miller indices or an indication for their maximum values. The computation of structure factors and intensities requires additional input of the unit cell contents in the form of a table containing the atomic number, the occupation factor and the co-ordinates for each of the individual atomic positions. The diffracted X-ray intensity calculations are based on scattering factors published by Cromer and Mann [10]. The routines are able to identify forbidden reflections and take account of the multiplicity of the powder lines. Finally the calculated X-ray intensities are corrected for Lorentz-polarization factors and converted to relative values attributing 100 to the most intense line. The output of the program consists of a tabular listing of *hkl*, *d*-spacings, 2θ values, structure factors and intensities. An option is provided to plot X-ray intensities against degrees 2θ, but no provisions are made yet to correct for temperature and absorption effects.

3.2. Materials

$Cr_{23}C_6$ was obtained from MRC company (no. 39 062010 71) as a 99.9% pure 325 mesh powder. The other $M_{23}C_6$ carbides used in this study were electrolytically extracted from commercial high-temperature alloys in a 10% HCl-methanol solution to which 2% tartaric acid was added in order to prevent the precipitation of tungsten and niobium in the form of oxides [11]. Table II lists the nominal composition of the alloys from which the carbides were extracted. Semiquantitative indications on the composition of the extracted precipitates were obtained from energy-dispersive X-ray spectroscopy on individual carbide particles on Be-grids in a Philips EM 300 transmission electron microscope. Fluorescence and absorption effects were estimated to be negligible considering the small thickness of the samples [12].

3.3. X-ray diffraction

Accurate asymmetric transmission and back-reflection X-ray powder diffractographs were recorded at room temperature with a Guinier camera of the Seemann–Bohlin focusing type using monochromatic Cr$K\alpha_1$ radiation. α-Quartz was added to the powders as an internal standard. The positions of all maxima were measured with a precision corresponding to $0.02°2\theta$. The scale of the film-measuring device was subsequently converted into a precise angular scale through a linear least-squares minimization of the difference between the measured and the theoretical quartz line positions. Upon averaging the lattice spacings obtained from each of the individual $M_{23}C_6$ lines, the standard deviation was smaller than 0.2 pm. Intensity measurements were performed by densitometry of the Guinier diffractographs using a Zeiss Jena micro-densitometer. The results were verified by visual comparison with the diffracted intensities of the calibration substance and by examination of Cr$K\bar{\alpha}$ diffractometer recordings.

4. Results and discussion

4.1. Calculations

4.1.1. Computation of diffraction patterns

The influence of the unit cell occupation on diffracted X-ray intensities was established by means of the computer program CRYDIF. For reference and in order to verify the procedure, the first pattern to be computed was that of pure $Cr_{23}C_6$. The positions of the atoms in the cell used as a basis for the calculations were taken from Pearson [13]. The resulting diffractograph is juxtaposed to the literature data in Fig. 2. The main characteristics of the computed pattern can clearly be recognized in most of the PDF patterns (Fig. 2a–d). For many lines, however, the PDF intensities are an order of magnitude higher than calculated. These deviations are ascribed to an overestimation of the intensities in the PDF patterns. In this respect it is recalled that the intensities under discussion are merely visual estimates from photographic recordings. It is thought that these values may have been influenced by the conditions of film exposure and development. Consistently, a PDF pattern of an analogous substance [14] recorded with a diffractometer corresponds much more closely to the calculated one. This observation furthermore confirms that the unit cell data are sufficiently accurate for the computer program to reproduce the diffractograph in full detail. The unit cell data for CRYDIF were subsequently modified so as to represent situations in which more heavily scattering atoms

TABLE II Composition of the investigated alloys (at.%) and lattice spacings of extracted carbides (nm)

Alloys		Composition														
		$M_{23}C_6$ forming elements							MC-forming			Other				
		Cr	Fe	W	Mo	C	at.x/at.Cr	$a_{M_{23}C_6}$ (nm)	Nb	Ti	a_{MC} (nm)	Ni	Co	Mn	Si	Al
Austenitic	1.4841	25	51	–	–	0.3	1.94	1.063	–	–	–	19	–	1.1	4	–
stainless	HK40	26	50	–	–	1.3	1.94	1.0631	–	–	–	20	–	0.6	2.6	–
steels	IN519	25	48	–	–	1.6	1.90	1.0628	0.9	–	0.444	22	–	0.7	1.5	–
	Incoloy 802	22	43	–	–	1.6	1.95	1.0630	–	0.9	0.433	30	–	0.75	0.75	1.2
Ni-base	Nimonic 75	21	4	–	–	0.5	0.23	1.0643	–	0.4	0.424	74	–	–	–	–
super-	IN 638	28.5	17	1.6	–	2.1	0.054	1.0677	0.6	–	0.444	34	14	0.4	1.1	–
alloys	Incoloy 807	22	23	1.6	–	0.4	0.070	1.0683	0.6	0.7	0.442	40	8	1	1.5	1
	IN 643	28	3	3	0.3	2.5	0.102	1.0699	1.3	0.1	0.442	49	12	–	0.6	–
	IN 738	17.5	0.5	0.9	1	0.5	0.106	1.0701	0.5 (Ta0.6)	4	0.437	60	8	–	–	7
	Waspaloy	21	0.1	–	2.5/2.7	0.2	0.118/0.128	1.0696/1.0711	–	3.5	0.433	56	14	0.04	0.1	2.6
	IN 100	10	–	–	1.8	0.8	0.161	1.0723	–	5	0.432	56	14	–	–	11

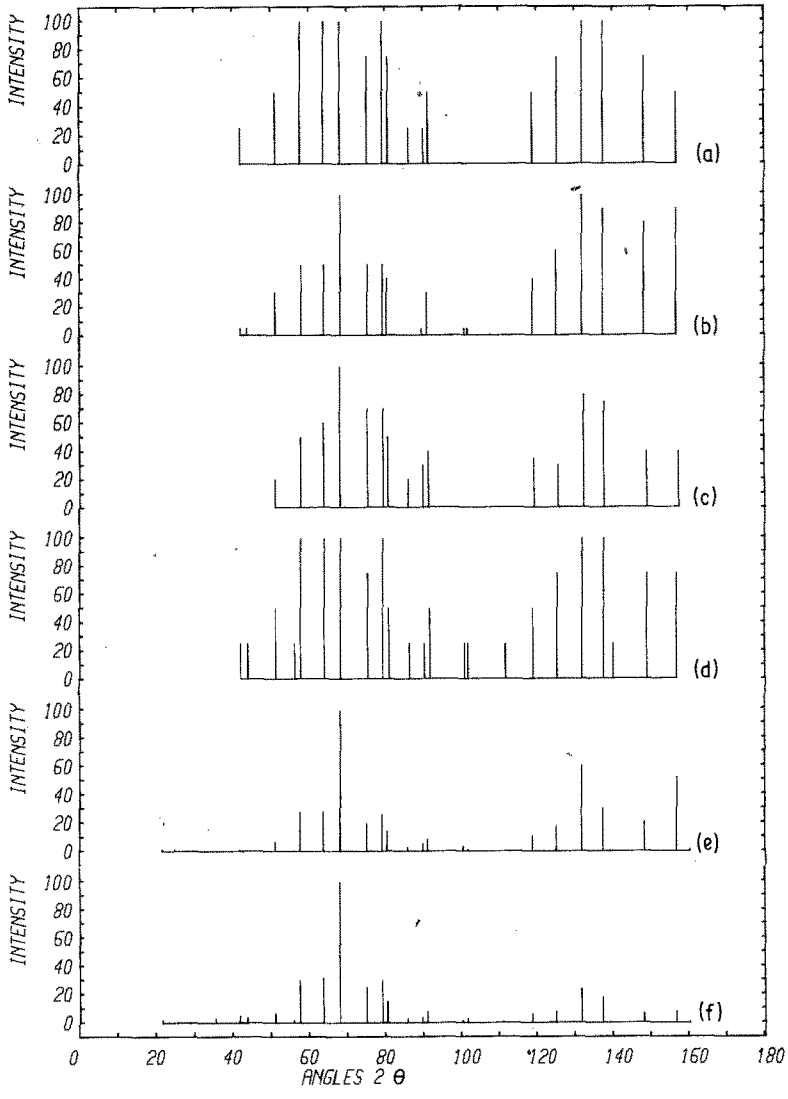

Figure 2 Cr$K\bar{\alpha}$ diffractographs of $Cr_{23}C_6$. Diffractographs according to (a) [5], (b) PDF 14-407, (c) PDF 11-545, (d) PDF 9-122, (e) calculations (not corrected for absorption).

replaced the Cr at various positions. The case where, contrary to Goldschmidts predictions, no preference for particular positions should exist, was simulated by randomly replacing Cr by W. This affected the intensities of all the reflections evenly, resulting in a pattern identical to that of pure $Cr_{23}C_6$.

Diffractographs calculated for $Cr_{23}C_6$ in which 10, 50 and 100% of the Cr-atoms on c-positions were randomly replaced by W are shown in Fig. 3. One notices that {400} and {840} gradually disappear and {200}, {220}, {420}, {422}, {620}, {622}, {642}, {820}, {622} and {842} become more intense. Only reflections with even indices are affected, which is in agreement with the specific point symmetry of the c-positions involved [15].

Fig. 3 further shows that the effect of less heavy atoms like Mo is similar, but smaller than that of W in the sense that the intensity distribution obtained on full substition by Mo corresponds to the one obtained on about 50% substitution by W.

Theoretical X-ray powder diffractographs of $M_{23}C_6$ with W occupying other particular positions than those predicted by Goldschmidt showed characteristic intensity changes which were quite different from those in Fig. 3.

When the described procedure was finally applied to investigate the effect of Fe and Ni, it indicated that the substitution of Cr by Fe or Ni

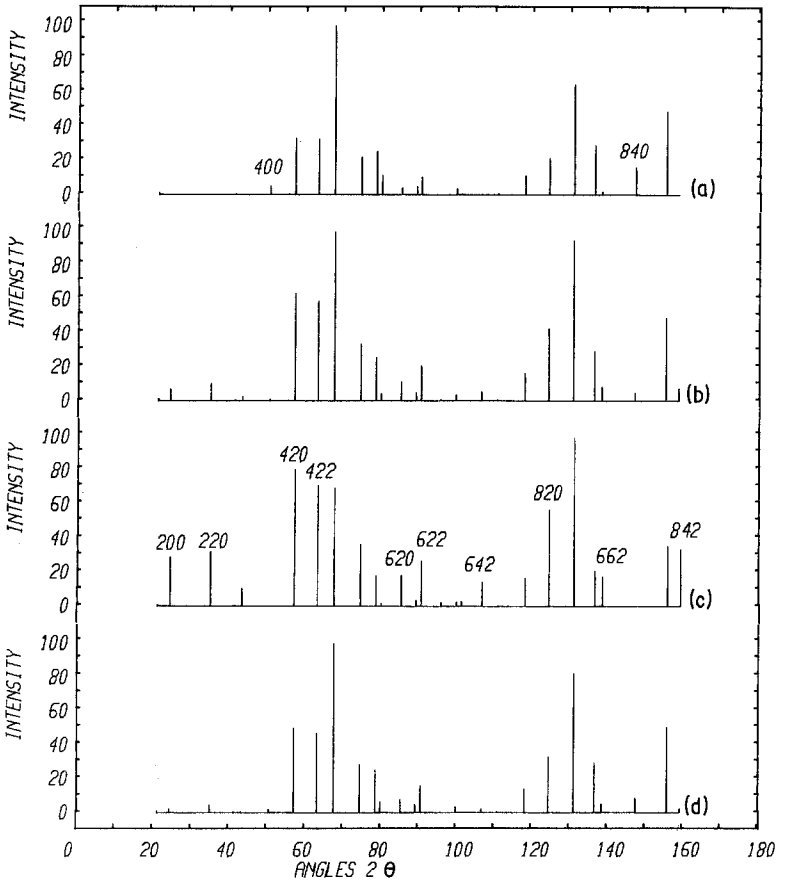

Figure 3 CrKα diffractographs computed for W and Mo containing $M_{23}C_6$. (a) 10%, (b) 50%, (c) All the Cr-atoms on c-positions replaced by W. (d) All the Cr-atoms on c-positions replaced by Mo, (f) experimental observation.

does not give rise to any intensity change susceptible to detection by powder diffraction techniques. This absence of readily measurable changes is due to the fact that the scattering factors of Fe and Ni are virtually equal to those of Cr.

4.1.2. Estimate of lattice constants

The incorporation of Fe, W or Mo into the lattice of $Cr_{23}C_6$ may not only affect the diffracted intensities, it will also modify the carbide's lattice constant. The sign and the magnitude of the changes depend mainly on the difference in atomic radius between chromium and the above metal atoms and on the number of lattice positions these atoms occupy. The interval within which the lattice parameters of the $(Cr, Fe, W, Mo)_{23}C_6$ carbides subject of the present study may fall, can roughly be estimated as follows.

W and Mo atoms are 10% larger than Cr (Table I) and may replace 8 out of 92, or 9%, of the metal atoms in the unit cell. If all the positions are occupied so as to form $Cr_{21}(W, Mo)_2C_6$, an increase of the lattice parameter to about $1.066 \times (1 + 0.1 \times 0.09) = 1.075$ nm should result. This value agrees well with the findings of Westgren who measured $a = 1.075$ nm for $Cr_{21}W_2C_6$ [1].

Fe atoms, on the other hand, are 1% smaller than Cr (Table I) and the unit cell may theoretically accommodate 32 of them, i.e. 35% of the total number of metal atoms, which will reduce the lattice constant to approximately $1.066 \times (1 - 0.01 \times 0.35) = 1.062$ nm. The measurements of Westgren *et al.* in fact revealed a more pronounced reduction to 1.059 nm for a carbide of the formula $Cr_{15}Fe_8C_6$ [16].

4.2. Experimental observations

4.2.1. Composition and lattice spacings

Except for pure $Cr_{23}C_6$, all the carbides described under this heading were extracted from the commercial high-temperature alloys mentioned in

TABLE III Relation between the composition of an alloy (in at.%) and the intensities in energy dispersive X-ray spectra of extracted M_{23} carbides. vs = 100, m = 25, w = 10, · = 5

Alloy						$M_{23}C_6$ extract					
	Ni	Cr	Fe	W	Mo	Ni	Cr	Fe	W	Mo	$a_{M_{23}C_6}$ (nm)
IN 519	22.5	25	48	–	–	·	vs	w	–	–	1.0628
Incoloy 807	40	22	23	1.6	–	w	vs	·	w	–	1.0683
IN 643	49.5	28	3	3	0.3	·	vs	–	m	·	1.0699
Waspaloy	56	21	2	–	2.5	·	vs	–	–	w	1.0696

Table II. The carbide constituents were identified by means of energy-dispersive X-ray spectroscopy. but the applied procedure did not allow a full quantitative analysis of the compositions to be made. Table III, therefore, gives only a semi-quantitative relationship between the carbide ingredients and the composition of the alloys in which the carbides formed.

The table shows that all the W and Mo containing alloys under examination grew typical (Cr, W/Mo)$_{23}C_6$ carbides, Fe was encountered whenever the alloys contained more than 25 at.% iron and, according to the high nickel content of all the alloys, Ni was found all over.

Accurate values for the lattice spacings of these carbides were obtained from Cr$K\alpha_1$ diffractographs. Pure $Cr_{23}C_6$ gave a value of 1.0658 ± 0.0001 nm which is in agreement with recent literature [17].

For the Cr, W, Mo carbides, the magnitude of the lattice constants tied up with the elemental composition of the parent alloys, following the trend set forward in Section 4.1.2. This is inferred from Table II which indicates how the parameters of the (Cr, W/Mo)$_{23}C_6$-type carbides increased with the number of W and/or Mo atoms per Cr atom in the host alloy. The saturation limit of 1.075 nm was not reached within the present set of alloys and the results suggest that a W, Mo/Cr atom ratio higher than about 0.25 would be required to do so. This extrapolation is supported by the findings of Donachie and Kriege who detected an $M_{23}C_6$ with a spacing of 1.075 nm in René 41 containing 0.28 Mo atoms per atom of Cr [11].

A different behaviour is encountered in (Cr, Fe)$_{23}C_6$-forming alloys. Extending from the values of 1.0658 nm for pure $Cr_{23}C_6$ and 1.064 nm for carbides in the 20Cr/5Fe alloy Nimonic 75 (Table II), one would expect 20Cr/40Fe austenitic stainless steels to grow fully substituted $Cr_{15}Fe_8C_6$ carbides with a lattice spacing < 1.062 nm (Section 4.1.2). The experiments, however, show that the spacing levels off at 1.063 nm pointing at an anomaly which will be given attention during further research.

4.2.2. Intensities in powder diffraction

Experimental data on the intensities and the positions of the diffraction maxima of pure $Cr_{23}C_6$ are compared to the literature data in Fig. 2. The present observations confirm that {200}, {444} and {642} are below the detection level of the powder diffraction method. {111}, {220}, {331}, {731}, {733}, {662} and {842}, on the contrary, could positively be identified, be it mostly as lines of low intensity.

Fig. 4 and Table IV show that the incorporation of Fe (and Ni) atoms into $Cr_{23}C_6$ does not noticeably affect the intensity distribution over the individual diffraction maxima. This absence of changes in the powder diffraction pattern is in accordance with theory, but unfortunately impedes further verification of Goldschmidt's predictions on the position of Fe atoms in $M_{23}C_6$, unless more sophisticated methods for intensity measurement and structure factor determination are involved.

Experiments on (Cr, W/Mo)$_{23}C_6$ finally prove that the introduction of W or Mo indeed modifies the diffracted intensity distribution of $Cr_{23}C_6$ (Fig. 4, Table IV). The lines {400} and {840} almost disappear whereas {200} and {642} appear and {220}, {420}, {422}, {620}, {820} and {822} see their intensities considerably increased. It is clear that only reflections with even indices *h*, *k* and *l* are affected and a comparison with Fig. 3 shows that the sign as well as the magnitude of the intensity changes correspond exactly to those computed for W and/or Mo on c-positions. No other unit cell configurations fit these observations. The experimental evidence thus fully supports Goldschmidt's predictions on the position of W and Mo in the lattice of $M_{23}C_6$.

5. Conclusions

(1) X-ray powder diffractographs of $Cr_{23}C_6$

TABLE IV Experimental values of the interplanar distances d_{hkl} and the intensities of the Cr$K\alpha$ X-ray diffraction peaks of $Cr_{23}C_6$, $(Cr, Fe)_{23}C_6$ and $(Cr, Fe, W)_{23}C_6$. The computed intensity values quoted in the last three columns have not been corrected for absorption

hkl	$Cr_{23}C_6$	$(Cr, Fe)_{23}C_6$	$(Cr, Fe, W)_{23}C_6$	$Cr_{23}C_6$	$(Cr, Fe)_{23}C_6$	$(Cr, Fe, W)_{23}C_6$	$Cr_{23}C_6$	$(Cr, Fe)_{23}C_6$	$(Cr, Fe, W)_{26}C_6$
	d_{hkl}	d_{hkl}	d_{hkl}	*I*	*I*	*I*	*I*	*I*	*I*
111	0.6157	0.6138	0.6164	2	6	4	1	0	1
200	–	–	0.5338	–	–	15	1	2	2
220	0.3769	–	0.3773	3	–	19	0	0	5
311	0.3213	0.3207	0.3220	5	6	5	1	2	1
222	0.3077	0.3069	0.3083	4	3	4	0	0	1
400	0.2664	0.2660	0.2669	7	6	(< 1)	7	9	2
331	0.2445	–	–	2	–	–	1	1	1
420	0.2384	0.2378	0.2387	30	25	68	28	27	50
422	0.2175	0.2171	0.2179	32	35	72	28	26	47
511	0.2051	0.2046	0.2055	100	100	100	100	100	100
440	0.1884	0.1880	0.1887	25	25	36	20	23	29
531	0.1801	0.1797	0.1804	30	20	20	26	28	26
600	0.1776	0.1772	0.1779	15	15	6	14	13	7
620	0.1685	0.1681	0.1688	3	4	12	3	3	8
533	0.1626	0.1622	0.1628	4	5	5	5	6	5
622	0.1607	0.1603	0.1609	8	8	18	8	8	16
444	–	–	0.1541	–	–	(< 1)	0	0	0
711	0.1494	0.1490	0.1496	2	3	1	4	4	4
640	0.1479	0.1476	0.1481	3	2	< 1	1	2	0
642	–	–	0.1428	–	–	5	0	0	2
731	0.1389	0.1384	–	1	1	–	1	1	1
800	0.1333	0.1329	0.1335	6	7	7	11	12	14
733	0.1303	0.1300	–	< 1	< 1	–	0	0	0
820	0.1293	0.1290	0.1295	8	8	20	18	19	34
822	0.1256	0.1253	0.1259	24	24	37	60	59	83
751	0.1231	0.1228	0.1233	18	18	17	30	32	30
662	0.1223	0.1219	0.1224	< 1	< 1	2	1	1	5
840	0.1192	0.1189	0.1194	7	7	< 1	21	27	9
911	0.1170	0.1167	0.1173	8	8	6	52	62	51
842	0.1163	0.1160	0.1165	1	1	1	2	1	2
a (nm)	1.0658	1.0631	1.0678						

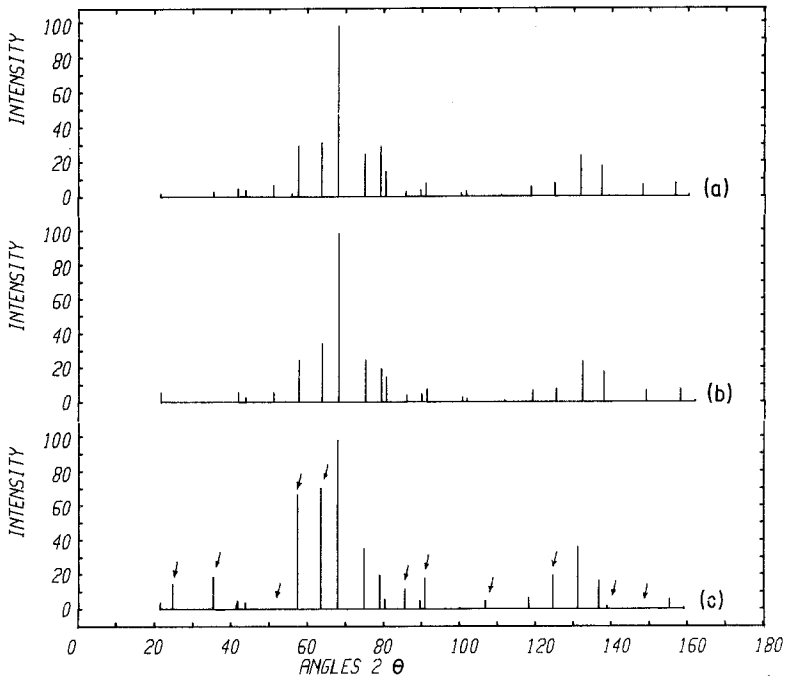

Figure 4 Experimental Cr$K\alpha$ X-ray diffractographs of (a) $Cr_{23}C_6$, (b) $(Cr, Fe)_{23}C_6$ and (c) $(Cr, Fe, W, Mo)_{23}C_6$.

recorded with Cr$K\alpha_1$ radiation in a modern focusing Guinier camera reveal more maxima than are actually mentioned in literature. The pattern comprises weak lines corresponding to {111}, {220} and {842}.

(2) The introduction of Fe into the lattice of $Cr_{23}C_6$ reduces the lattice constant but does not measurably affect the intensity distribution in the diffraction pattern.

(3) The incorporation of W or Mo increases the lattice constant of $M_{23}C_6$ and changes the diffracted intensities. All but the lines with uneven Miller indices see their intensities affected.

(4) This behaviour is explained by the fact that the heavy atoms occupy c-positions in the unit cell.

References

1. A. WESTGREN, *Jernkontorets Ann.* **117** (1933) 501.
2. G. WALLWORK and J. CROLL, *Rev. High-Temp. Mater.* **III(2)** (1976) 69.
3. G. S. UPADHYAYA, *ibid.* **III(1)** (1975) 25.
4. H. J. GOLDSCHMIDT, "Interstitial Alloys" (Butterwords, London, 1967).
5. A. WESTGREN and G. PHRAGMEN, *Kungl. Svensk. Vetensk. Handl.* **3(2)** (1926) 3.
6. A. WESTGREN, *Jernkontorets Ann.* **119** (1935) 231; PDF 9-122.
7. H. LUX and L. EBERLE, *Chem. Ber.* **94** (1961) 1562; PDF 14-407.
8. BEATTIE and VERSNYDER, *Trans. Amer. Soc. Met.* **49** (1957) 883; PDF 11-545.
9. JCPDS – International Centre for Diffraction data, 1601 Park Lane, Swarthmore, Pennsylvania 19081.
10. D. T. CROMER and J. B. MANN, *Acta Cryst.* **A24** (1968) 321.
11. M. J. DONACHIE and O. H. KRIEGE, *J. Mater.* 7 (1972) 269.
12. S. REED, in "Analysis of High Temperature Materials", (Applied Science Publishers, London, 1982).
13. W. B. PEARSON, "Lattice spacings and structures of metals and alloys", Vols. I and II (Pergamon Press, Oxford, 1964, 1967).
14. K. G. CARROLL, L. S. DARKEN, E. W. FILER and L. ZWELL, *Nature* **174** (1954) 978; PDF 12-570.
15. "International Tables for X-ray Crystallography" Vol. 1, edited by N. F. M. Henry and K. Lonsdale (Kynoch Press, Birmingham, 1962).
16. A. WESTGREN, G. PHRAGMEN and T. NEGRESCO, *J. Iron Steel Inst.* **117** (1926) 383.
17. E. ERDOS, in "Analysis of High Temperature Materials", (Applied Science Publishers, London, 1982).
18. R. C. EVANS, "An Introduction to Crystal Chemistry" (University Press, Cambridge, 1966).

Received 19 October 1981
and accepted 8 March 1982